Indonesian Journal of Electrical Engineering and Computer Science
Vol. 41, No. 1, January 2026, pp. 309~319
ISSN: 2502-4752, DOI: 10.11591/ijeecs.v41.i1.pp309-319

Lung cancer segmentation and classification using hybrid CNN-LSTM model

Manaswini Pradhan[1], Ahmed Alkhayyat[2,3,4]
[1]P.G. Department of Computer Science, Fakir Mohan University, Balasore, India
[2]College of Technical Engineering, Islamic University, Najaf, Iraq
[3]College of Technical Engineering, Islamic University of Al Diwaniyah, Al Diwaniyah, Iraq
[4]College of Technical Engineering, Islamic University of Babylon, Babylon, Iraq

Article Info

Article history:

Received Jan 25, 2024
Revised Nov 13, 2025
Accepted Dec 13, 2025

Keywords:

Computed tomography
Convolutional neural network
Lung cancer
Nodules
Segmentation

ABSTRACT

A collection of genetic disorders and various types of abnormalities in the metabolism lead to cancer, a fatal disease. Lung and colon cancer are found to be main causes of death and infirmity in people. When choosing the best course of treatment, the diagnosis of these tumors is usually the most important consideration. This study's main objectives are to classify lung cancer and its severity, as well as to recognize malignant lung nodules. The suggested approach additionally classifies the stages of lung cancer in order to recognize lung nodules. The convolutional neural network (CNN) is used to detect lung nodules, identifying a nodule which is accurately segmented and classified. The suggested method is separated into dual parts: primarily, it classifies normal and abnormal behavior, and the subsequent one classifies the different stages of lung cancer. Texture and intensity-based features are extracted during the classification stage. When compared to other methods such as nested long short-term memory (LSTM)+ CNN, the hybrid CNN-LSTM obtains superior outcomes in terms of accuracy (99.35%), specificity (99.30%), sensitivity (99.32%), and F1-score (99.29%).

Corresponding Author:

Manaswini Pradhan
P.G. Department of Computer Science, Fakir Mohan University
Balasore, Odisha, India
Email: mpradhan.fmu@gmail.com

1. INTRODUCTION

Due to the combination of various varieties of abnormalities in biochemical and genetic diseases, the dangerous lung cancer and colon diseases are caused. It is difficult to understand the disease's nature for segmentation and categorization of medical images accurately [1]. Computed tomography (CT) and magnetic resonance (MR) of automatic segmentation of images achieve popularity [2]. Lung cancer is a very dangerous disease which leads to death and offer poor predictions [3]. Various approaches are exploited during the early phase detection of lung cancer, which comprises CT scans, magnetic resonance imaging (MRI) and X-rays [4]. Convolutional neural network (CNN) algorithms are proven to be more efficient at generating better sensitivity and reduced false positive detection rates [5]. Lung cancer is the uncontrolled distribution of cells in the lung area. A difficulty in breathing is also brought on by lung cancer. Lung cancers of non-small cells and small cells are among the several types of the disease. Early detection of lung cancer is essential for lowering death rates [6]. Machine learning (ML) classifiers estimate the diagnosis of lung cancer patients using extracted image characteristics automatically from WSIs, contributing to precision oncology [7]. Advanced results for image detection, segmentation, and classification are achieved using deep learning (DL) based approaches [8]. The images from CT scans and positron emission tomography (PET) are the best

ways for identifying the lung tissue region while developing cancer [9]. The sophisticated models resolve and enhance the entire process of detecting lung cancer [10]. A multilayer brightness-preserving approach has been exploited to frequently analyze the desired CT lung images to enhance the quality of lung image [11].

For segmentation and detection, the efficient low-level vector quantization (VQ) is engaged to detect initial nodule candidates (INCs) inside the lung, which is computationally proficient when compared to the current approaches [12]. To lower the false-positive (FP) rate, feature-based support vector machine (SVM) is used in conjunction with rule-based filtering [13]. MediNet is a visual dataset for transfer learning (TL) applications that solely contain medical images. For the Covid-19, diabetic retinopathy and chest datafiles, all learning algorithm transfers are retrained using the fine-tuning approach, and the feature sets and weight vectors are then utilized to detect diseases [14]. To provide the algorithm with a massive data file containing all possible cancer cases in order to accurately classify colon and lung cancer. To enhance cancer classification efficiency, an ensemble approach is employed [15]. the dual-tree m-band wavelet transform (DTWT) is exploited to CT pictures which is implemented by Priya and Venkatesan [16]. At both higher and lower frequencies, it produces sub-band coefficients. After that, low-frequency components are reset to zero. This approach uses an SVM to accomplish superior prediction accuracy, which improves the system performance. Then, reconstruction is carried out by employing components with higher frequencies. Unfortunately, one abnormal image is mistakenly categorized using an SVM classifier by the conducted procedure. Naïve Bayes with cuckoo search optimization were used by Manickavasagam and Selvan [17] to improve sensitivity and the accuracy of lung cancer. This method has the advantage of producing better results and efficient training without requiring a large trial size of data files. On the other hand, the suggested method reduces the sensitivity of nodule identification, diminishing the results.

MediNet and RdiNet were implemented by Reis *et al.* [18] which included the 10-class new visual datafile known as MediNet. The RdiNet DL algorithm was implemented and used in TL applications for pre-training and classification. To achieve good results, the implemented method MediNet made use of a small dataset. Furthermore, it showed that the superior results are obtained in the medical industry when TL techniques are applied. To improve the success rate of the TL approach, the MediNet's ten categories and smaller sample size of data should be increased. A hybrid group approach of feature extraction was used by Talukder *et al.* [19] to successfully identify lung and colon cancer. Civit-Masot *et al.* [20] developed a CNN for the diagnosis of lung cancer. The evaluation of the variations in effective classification results was caused by the addition of different strategies. This method increased false negative by decreasing precision, sensitivity, and accuracy. From the above literature survey, the overall limitations are taken from reference papers using an SVM classifier which erroneously identified an anomalous image, and the cuckoo search optimization reduced the sensitivity of nodules identification. MediNet framed a small number of data as the single feature extractor cannot deliver consistent results. To overcome these problems, a combined strategy which increased the success rate of classification to the TL rate is required. This paper identified certain limitations where the extraction of a single feature led to inadequately consistent outcomes. The proposed method was suitable for classifying one abnormal image, lowered the sensitivity of node identification, reduced the precision and sensitivity, and also increased the false negative. To reduce these limitations, the new model is used to overcome the good classification result, increase sensitivity and precision, and also used to decrease the false negative in the future work. The contributions are listed as follows:

i) A hybrid CNN-LSTM network is incorporated to assist in the automatic initial determination of lung cancer patients.
ii) The performance of the technique used is measured using the receiver operating characteristic (ROC), and an extensive evaluation of the study's results is provided in terms of performance measures.

The structure of this article is arranged as follows: section 2 explains the proposed method. section 3 represents the process of CNN-long short term memory (LSTM), and section 4 explains the results and discussion, while section 5 describes the conclusion.

2. PROPOSED METHOD

The classification of lung diseases and their general structure is depicted in the Figure 1. In the proposed method, feature extraction techniques and ML models are used to predict lung cancer and colon by utilizing lung histopathology and LC25000 colon image databases. To improve segmentation and classification in the specified query image, the proposed method is introduced as it achieves the highest sensitivity, accuracy, specificity and F1-score is demonstrated in this setup. The ideal representation of block diagram of the developed system is given in Figure 1.

For identifying lung cancer, a greater number of classification phases are included in the proposed method such as pre-processing, feature extraction, feeding into ML, TL, evaluation of the performance, and

high-performance filter are used for lung cancer classification based on the query image. The measures like accuracy, specificity, and F1-score are exploited to assess CNN-LSTM's performance.

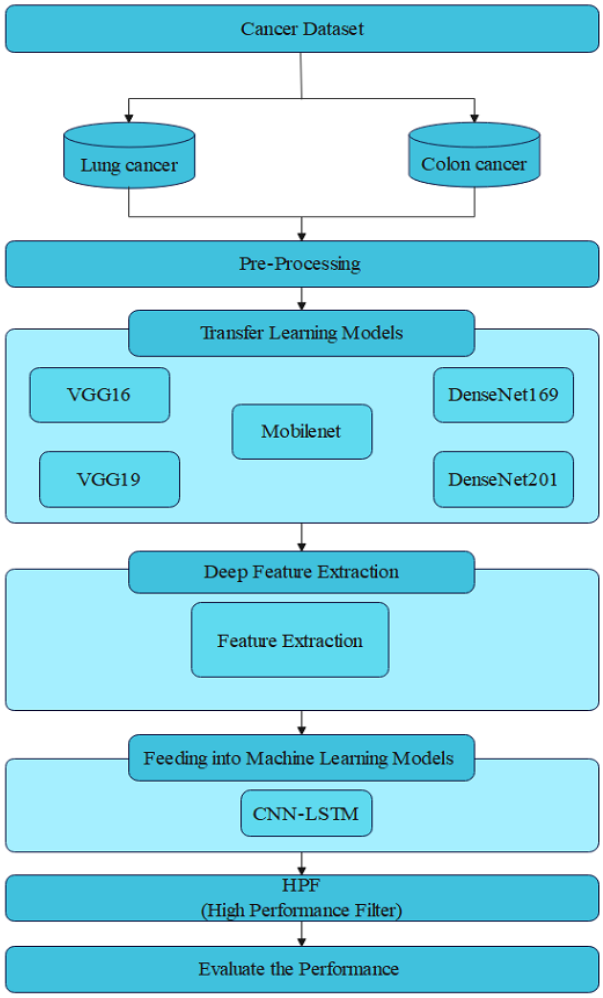

Figure 1. Block diagram for developed system

2.1. Dataset

In this research paper, lung cancer and colon datasets of histopathological (LC25000) [21] images are used to classify the query image and there are 25,000 images in both the datasets. Out of them, 15,000 images are from lung cancer dataset and 10,000 images are from colon cancer. In lung cancer, there are 3 classes in cell labels namely, adenocarcinomas, benignant tissue, and squamous cell carcinomas, and in colon, there are 2 classes in cell labels namely, benign tissue and adenocarcinomas. Initially, there are 750 images of lung tissue, and from that, 250 images are squamous cell carcinomas, 250 images are adenocarcinomas, and 250 are benign, and these sample images are enhanced to produce 25,000 images. The LC25000 dataset are a sample of confirmed reference and HIPAA-compliant. In this proposed system, from 25,000 images of both colon and lung cancer images, only 10,000 images are used for classification and prediction of lung cancer disease. From the 10,000 images, 4,200 and 2,800 images are in the combination of both lung and colon, respectively, and 5,000 images are of colon tissues.

2.2. Pre-processing of dataset

Pre-processing of images in the dataset [22] gives brighter, clearer, and more detail-rich than the original, making them suited for driving into models and achieving higher performance of the images. In convolutional kernel matrix, weighted average of each pixel surrounding its neighborhood is given by using convolutional filter. Various visual effects are evolved by different kernel's shape and size. Mathematically, the operation in convolutional is expressed as shown below.

Let us assume, $I = I(i,j)_{j=1,\ldots,M}^{i=1,\ldots,N}$ is a grayscale image. Consider the convolutional matrix of the kernel as $M = M(k,l)_{l=1,\ldots,q}^{k=1,\ldots,p}$, where it uses n and m integers as non-negative in $p = 2n+1, q = 2m+1$. When convolutional, M is applied for the query image I, and produces the outcome as $\mathrm{I}' = \mathrm{I}'(i,j)_{j=1,\ldots,M}^{i=1,\ldots N}$ where each (x0, y0) is expressed in (1).

$$I'(x_0, y_0) = \sum_{a=-n}^{n} \sum_{b=-m}^{m} M(a,b)\, I(x_0 + a, y_0 + b) \quad (1)$$

Where, $1 \leq x_0 - n, x_0 + n \leq N, 1 \leq y_0 - m, y_0 + m \leq M$.

2.3. Transfer learning models

For analyzing the dataset and extracting features, the proposed method uses five TL models such as MobileNet, DenseNet, 201VGG19, visual geometry group-16 (VGG16), and DenseNet201. ML approaches are exploited to assess the performance of CNN-LSTM.

i) VGG16: the cores of gigger convolutional are replaced by 33 multiple convolutional cores in AlexNet are enhanced by VGG16, and [23] causes decrease in the number of parameters and increase in the network depth. Convolutional, fully linked layers, and pooling are the three components of VGG16 TL. The convolutional layer uses filters to retrieve the information present in images; the two significant characteristics are size of stride and kernel, while the poling layer reduces dimensionality and computations while increasing the spatial density of the network. They interact with the lower levels in completely linked layers in a fully connected manner.
ii) VGG19: the VGG19 [24] model consists of 19 layers and is a feature extractor of weighted ground. For the classification of the images into various 1,000 classes 3 dense layers and 16 convolutional layers are combined. VGG19 was implemented by using ImageNet which contains million number of images and are classified into 1,000 classes. There are 4 conv 1 max pool, 3 FC layers, 2 conv 1 max pool in proposed method. As it employs 3x3 multiple filters convent, it is popular for photo prediction model.
iii) MobileNet: pointwise and depthwise convolutions are the two layers presented in MobileNet. To minimalize computational cost in preliminary few layers, separable depthwise convolutions are introduced, while depthwise convolutions are used to allocate various filters of input in every class, and to develop a joint distribution, conv 1x1 (pointwise) is used in output of depthwise layers. After every convolutional rectified linear unit (ReLU), and batch normalized (BN) is used. The accuracy trade-off and delay calculate the efficiency, and are used to identify, segment, and categorize the images.
iv) DenseNet: DenseNet feeds forward every layer and effects the behavior of each continuous layer, known as the CNN. There are a total of five layers in the DenseNet block, out of which the initial 4 layers are thick and last layer is the transition layer; here, k is the rate of growth in every layer. 2x2 through a 2 stride and conv 1x1 is the average pool of transition layer if the rate of growth is 4, while 1x1 of 3x3 with 1 stride and conv are in four layers. DenseNet169, DenseNet networks, and DenseNet201 are used in CNN-LSTM model for performance evaluation.

2.4. Deep feature extraction

Different current models are used and modified in this experiment so as to meet the requirements as more attention was drawn by the proposed DL approach. To retrieve the specific attributes in the dataset, it separates only few layers and uses the trained weights in the frozen layer, instead of training total model. Significant features in images play a major role in effective identification of the images.

Feature extraction: this process is exploited to extract features from max-pooling of the last block layer of an FC layer. The input image size is 128×128×3, before and after feature shapes are used in the feature extraction procedure. After feature extraction, the feature's final size is 16,384. At this point, n refers number of input images; further, input/output feature sizes for colon, lung, and other cancers are calculated. The extracted characteristics are provided to the ML algorithm to evaluate each ML model's effectiveness. All of the TL models are applied using this method.

3. CONVOLUTIONAL NEURAL NETWORK AND LONG SHORT-TERM MEMORY

3.1. Convolutional neural network

In the proposed method, many filters are used to train the image at different phases by using CNN to identify different properties of an image. The main aim of CNN is to retrieve local characteristics from higher-level and processed to a lower-level. Each layer output is taken as input for next layers that starts with the straightforward properties like edges, brightness and finds it more difficult when classifying each item particularly. CNN consists of SoftMax layer, ReLU, convolutional layer, pooling layers, dense, and fully

connected (FC). To demonstrate the feature maps mass, convolutional layer kernels are used. It uses "stride(s)" to convolve a total input and by that, the measurements of outcome value come as an integer. Padding a volume input with zero is done by using zero padding and continue its dimensions with features of the lower-level. The working of convolutional layer is written in the (2).

$$F\ (i,j)\ =\ (I\ *\ K)\ (i,j)\ =\ \sum\sum I(i+m,j+n)K(m,n) \tag{2}$$

In the (2), the feature map outcome is denoted by F, input matrix is denoted by I, convolutional layer working is denoted by $I * K$, $m * n$ is the size of 2D filter which is represented by K. By keeping input threshold value as zero, ReLU activation is computed and mathematically given as in (3),

$$f(x)\ =\ max\ (0,x) \tag{3}$$

3.2. Long short-term memory

LSTM consists of single input points, while feedback line present in LSTM is used to manage full data sequence. LSTM is together with 3 gates namely, input, output, and forget; here, x_t refers to the current input, and h_{t-1} and h_t refer to the current and previous output, and new and prior states of cells are denoted by C_{t-1} and $\widetilde{C_t}$, correspondingly.

LSTM input gate is demonstrated in (4)-(6).

$$i_t = \sigma(W_i.[h_{t-1},x_t] + b_i) \tag{4}$$

$$\widetilde{C_t} = tanh(W_i.[h_{t-1},x_t] + b_i) \tag{5}$$

$$C_t = f_t\ C_{t-1} + i_t\widetilde{C_t} \tag{6}$$

Sigmoid layer is utilized to determine which part of data to be considered by following h_{t-1} and x_t, and is used in (4). To enhance the data h_{t-1} , x_t and h_{t-1} should move with the layer of tanh in (5). The current instant, $\widetilde{C_t}$ and long-term memory in data is in (6), where W_i is defined by the output of the sigmoid, the output of tanh is denoted by $\widetilde{C_t}$, here $\widetilde{C_t}$ is converted by C_{t-1}. LSTM input gate bias is denoted by b_i, and weight matrices are defined as W_f. For the selective transmission of data the sigmoid layer and dot product together with the LSTM is permitted by the forget gate. Here in (7), the offset is referred to as b_f, weight matrix is symbolized as W_f, and sigmoid function is represented by σ, that is exploited to determine the forget data matched with a specific probability from the earlier stage or not.

$$f_t = \sigma(W_f.[h_{t-1},x_t] + b_f) \tag{7}$$

The necessary states for the inputs of h_{t-1} and x_t are calculated by the LSTM's, as shown in the (8) and (9). C_t is the new information that is carried by the decision vectors, and to generate final output $tanh$ function is retrieved and multiplied.

$$O_t = \sigma(W_o.[h_{t-1},x_t] + b_o) \tag{8}$$

$$h_t = O_t tanh(C_t) \tag{9}$$

Where, b_o and W_o denote the bias and weighted matrices.

3.3. Hybrid CNN-LSTM

An LSTM architecture known as CNN-LSTM is created particularly for the process prediction issues including visual inputs like images or videos. For identifying lung cancer instances automatically, three kinds of images of X-rays are used in this combination system. The structure of the architecture is developed by fusing networks of LSTM and CNN, as classifiers CNN are used to remove the complex details from LSTM and images functions.

The proposed hybrid network is used to detect the lung cancer disease as shown in Figure 2. The network of 20 layers: 5 pooling layers, 12 layers of convolutional, 1 layer of LSTM, 1 output layer, and 1 layer of FC with a function SoftMax. Two or three 2D CNNs, a pooling layer, and a convolutional layer are combined to create 25% rate of dropout of every dropout layer and convolutional block. The convolutional layer is activated by using ReLU function, which has a 3x3 kernel size for feature extraction. The 2x2 kernels

is the dimension of max-pooling layer which minimizes the size of the input image. The map function is sent to the layer LSTM in the best section of the architecture to extract time data. (none,7,7,512) is the output shape discovered by following the convolutional block. The LSTM input size is enhanced (49,512) using reshape approach. The design classifies the image X-ray over a completely linked layer after analyzing the time characteristics to determine which of the three categories (normal, lung cancer, and pneumonia) they belong with. For difficult classification issues combination of CNN-LSTM method is utilized.

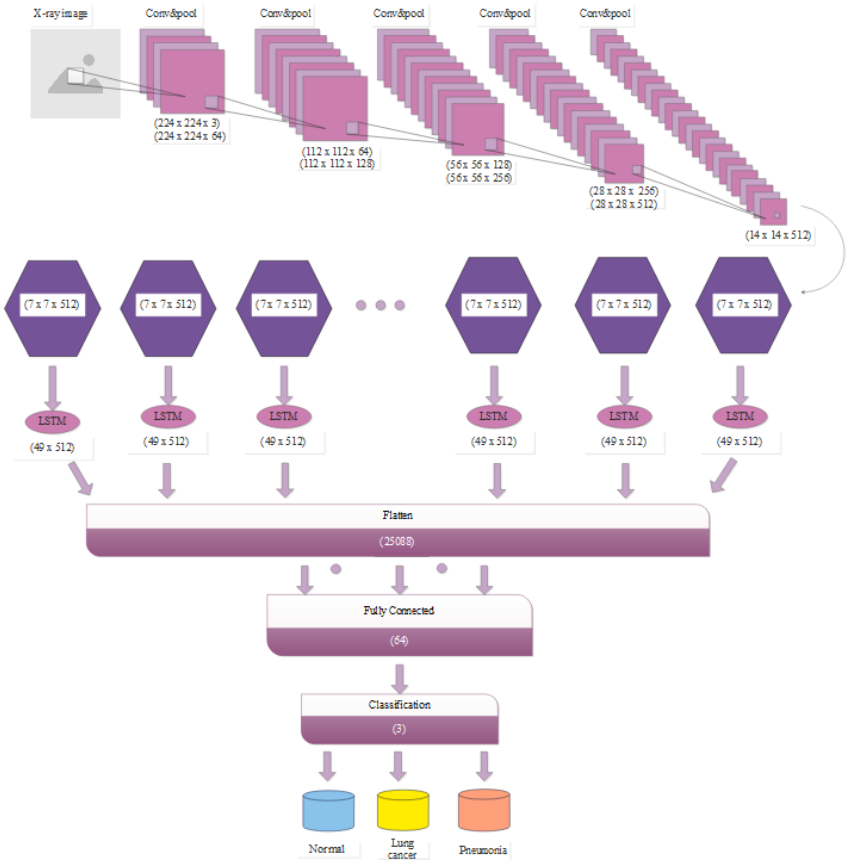

Figure 2. A demonstration of the implemented hybrid network for lung cancer classification

3.4. High performance filter

The ML algorithms of the top three fill input into the ensemble learning procedure using a mechanism called high-performance filtering (HPF) [25]. Finding the estimators that fill input into the method of ensemble learning to get the final output, is the result of this HPF procedure. HPF in conjunction with ensemble learning is used to evaluate the way of implemented model performs. In this analysis, the number of performance metrics including specificity, sensitivity, F1-score, confusion matrix, and accuracy. The proposed framework's classifier algorithms have an accuracy rate of over 99% for the detection of colon and lung cancer.

4. RESULTS AND DISCUSSION

This section examines the performance of various TL methods. It then looks at the hybrid method which incorporates a classifier voting model and a high-performance TL model. This study shows that the MobileNet model performs better than each of the other TL models.

4.1. Analysis of lung cancer

A number of soft and hard voting classifier results of several TL models are displayed in Table 1. From those results, MobileNet outperforms other average models with accuracy values. Furthermore, MobileNet comprises a higher rate than the remaining models and the suggested model uses MobileNet in its lung cancer dataset.

Table 1. Evaluation of accuracy using TL

TL	VGG16 (%)	VGG19 (%)	MobileNet (%)	DenseNet169 (%)	DenseNet201 (%)
Hard	98.7	98.89	99.89	98.77	99.66
Soft	98.99	99.24	99.78	99.19	99.91
Average	98.83	98.89	99.84	98.96	99.77

4.2. Analysis of colon

Additionally, Table 2 illustrates the evaluation of accuracy using TL. These positive findings are made possible by effective feature extraction, ensemble soft voting classifiers, and appropriate pre-processing. The accuracy label for the MobileNet model obtains its greatest level ever, since it provides greater feature extraction than other TL models. A model is stronger and more effective if it receives predictions from several models rather than just one. Because of this, the ensemble approach was employed to obtain high-performance outcomes.

Table 2. Evaluation of accuracy using TL

TL	VGG16	VGG19	MobileNet	DendeNet169	DenseNet201
Hard	99.80	99.61	99.78	99.69	99.79
Soft	99.80	99.61	99.78	99.69	99.79
Average	99.80	99.61	99.78	99.69	99.79

4.3. Analysis of lung and colon

Table 3 and Figure 3 represents the performance of various TL models and shows that the model TL of MobileNet results superior on different average order models of TL. The accuracy rate on lung and colon values is about 98.81%, 99.35%, 99.32%, 99.31%, and 99.12% for VGG19, VGG16, MobileNet, DenseNet201, and DenseNet169.

Table 3. Evaluation of accuracy using TL models

TL	VGG16	VGG19	MobileNet	DeseNet169	DenseNet201
Hard	99.3	98.52	99.3	98.75	99.27
Soft	99.4	99.1	99.35	99.5	99.35
Average	99.35	98.81	99.32	99.12	99.31

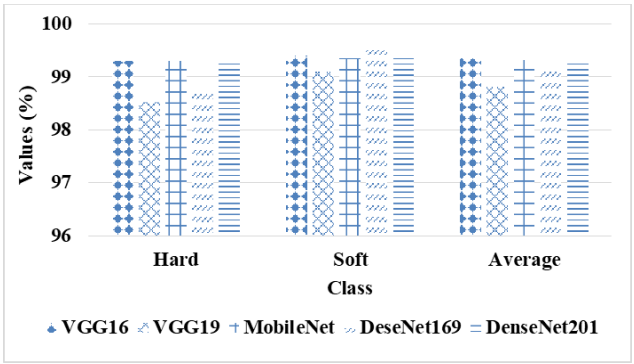

Figure 3. Accuracy evaluation on lung and cancer dataset

4.4. Performance analysis of CNN-LSTM classification

The confusion matrix of the CNN competitive and implemented structure of LSTM for classification of lung cancer is shown in Figure 4. The CNN architecture incorrectly identifies the 14 images out of the 915, including three for lung cancer. Only eight images, and two images for lung cancer were incorrectly categorized using the proposed LSTM model. It is discovered that the implemented network of LSTM outperforms the rival network of CNN since it contains greater true negative and positive values along with fewer values of false positive values and false negative. The lung cancer instances are effectively classified using the implemented approach as a result.

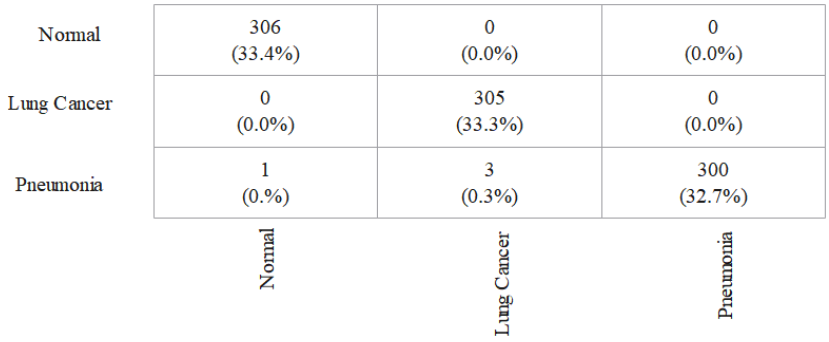

Figure 4. Confusion matrix of the proposed lung cancer detection system

Additionally, evaluating the performance of CNN classifier's cross-entropy (loss) and accuracy during the validation and training phases is also shown. At epoch 125, the accuracy for validation and training is 94.4% and 96.7%, respectively. Similar to this, the architecture of CNN has a loss of validation of 0.26 and a loss of training of 0.09. Moreover, a visual representation of the cross-entropy (loss) and accuracy performance evaluations of the LSTN classifier during the phases of training and validation is given. At epoch 125, the achieved accuracy for validation and training is respectively 97.0% and 98.3%. The LSTM architecture correspondingly has validation and training losses of 0.07 and 0.05. When compared to the architecture of CNN, the LSTM architecture produces higher training and validation accuracy ratings. The performance measures for each CNN are shown graphically in Table 4 and Figure 5.

Table 4. Assessment of CNN model

Class	Accuracy (%)	Specificity (%)	Sensitivity (%)	F1-score (%)
Normal	99.9	98.9	100	98.6
Pneumonia	98.6	99.9	97.8	98.7
Lung cancer	98.5	98.7	99.5	98.9

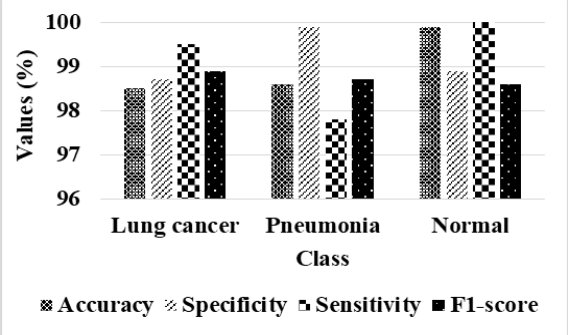

Figure 5. Graphical representation of CNN results

Table 5 and Figure 6 display the operation features for each class of the CNN+LSTM process. Although the sensitivity of 99.6% suggests that false negatives are inadequate, the specificity of 99.5% suggests the total number of true negatives is excessive. For pneumonia, it gains 98.4% sensitivity, 99.2% F1-score, and 99.8% specificity. For the typical cases, it accomplishes 100% sensitivity, 99.8% specificity, and 99.8% F1-score.

Table 5. Assessment of CNN-LSTM network

Class	Accuracy (%)	Specificity (%)	Sensitivity (%)	F1-score (%)
Normal	99.3	99.8	100	99.8
Pneumonia	99.5	99.8	98.4	99.2
Lung cancer	99.9	99.5	99.6	98.9

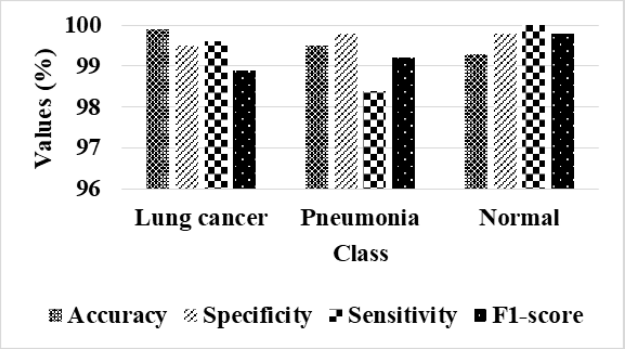

Figure 6. Graphical illustration of CNN-LSTM

Moreover, the false positive rate (FPR) and true positive rate (TPR) ROC curves are combined to assess the overall performance. It is evident that the network proposed outperforms the architecture of CNN since its area under the ROC curve (AUC) is determined have values with CNN of 99.8% design, and 99.9% for the architecture of CNN-LSTM. According to the results of the study, the CNN obtains 98.2% specificity, 95.3% AUC, and 97.7% F1-score for patients with lung cancer. The evaluations of results show that CNN+LSTM accomplishes an average specificity of 99.2%, an AUC of 99.9%, an F1-score of 98.9%, and a sensitivity of 99.3%. Finally, the heat map used to illustrate the experiment utilizing a target concept's gradients which is called gradient-weighted class activation mapping (Grad-CAM). A rough localization map indicates the key areas of images that are used for prediction once it has passed through the final layer.

The comparison of the suggested method with the current methods is shown in Table 6. The suggested model is assessed using the current techniques, such as those found in [18]-[20]. The recommended approach executes superiorly then the previous approaches which include CNN, hybrid, and nested LSTM+CNN designs. The most accurate model is the suggested CNN+LSTM when compared to above stated models.

Table 6. The implemented system comparison with extant systems

Model	Accuracy (%)	Specificity (%)	Sensitivity (%)	F1-score (%)
Nested LSTM+CNN [18]	80	74	81	77
Hybrid model custom CNN [19]	99.30	99.27	99.27	99.26
CNN [20]	97.11	97.15	97.13	97.14
CNN+LSTM	99.35	99.30	99.32	99.29

5. CONCLUSION

This study introduces a hybrid model for diagnosing lung and colon cancer that combines group learning models, k-fold, various TL models, specialized ML models, and HPF to select the best approach. In addition, MobileNet TL, DeseNet201, DenseNet169, VGG19, and VGG16 models are employed for feature extraction. A widespread DL model called CNN+LSTM is used as a hybrid system to assess performance. This study demonstrates that, when applied to the LC25000 dataset of lung and colon images, the hybrid method is efficient in identification. The CNN-LSTM accomplishes superior outcomes in terms of accuracy, specificity, sensitivity, and F1-score of approximately 99.35%, 99.30%, 99.32%, and 99.29%, correspondingly. Clinics may employ the suggested model for automated identification of lung cancer in the future. In order to improve the effectiveness of lung and colon cancer detection, the datasets for these two types of cancer should be investigated jointly in the future using an efficient DL technique.

FUNDING INFORMATION

The research described in this article involve no fundings from any agency.

AUTHOR CONTRIBUTIONS STATEMENT

This journal uses the Contributor Roles Taxonomy (CRediT) to recognize individual author contributions, reduce authorship disputes, and facilitate collaboration.

Name of Author	C	M	So	Va	Fo	I	R	D	O	E	Vi	Su	P	Fu
Manaswini Pradhan	✓	✓	✓	✓	✓	✓	✓	✓	✓	✓	✓	✓	✓	
Ahmed Alkhayyat											✓	✓	✓	

C : **C**onceptualization
M : **M**ethodology
So : **So**ftware
Va : **Va**lidation
Fo : **Fo**rmal analysis
I : **I**nvestigation
R : **R**esources
D : **D**ata Curation
O : Writing - **O**riginal Draft
E : Writing - Review & **E**diting
Vi : **Vi**sualization
Su : **Su**pervision
P : **P**roject administration
Fu : **Fu**nding acquisition

CONFLICT OF INTEREST STATEMENT

The authors declare no conflict of interest.

DATA AVAILABILITY

The lung cancer and colon datasets of histopathological (LC25000) [21] images are used to classify the query image and there are 25,000 images in both the datasets. Out of them, 15,000 images are from lung cancer dataset and 10,000 images are from colon cancer.

REFERENCES

[1] Y. Cao *et al.*, "Segmentation of lung cancer-caused metastatic lesions in bone scan images using self-defined model with deep supervision," *Biomedical Signal Processing and Control*, vol. 79, no. 1, p. 104068, Jan. 2023, doi: 10.1016/j.bspc.2022.104068.

[2] H. Yang *et al.*, "Deep learning-based six-type classifier for lung cancer and mimics from histopathological whole slide images: a retrospective study," *BMC Medicine*, vol. 19, no. 1, 2021, doi: 10.1186/s12916-021-01953-2.

[3] T. Meraj *et al.*, "Lung nodules detection using semantic segmentation and classification with optimal features," *Neural Computing and Applications*, vol. 33, no. 17, pp. 10737–10750, Sep. 2021, doi: 10.1007/s00521-020-04870-2.

[4] D. Gu, G. Liu, and Z. Xue, "On the performance of lung nodule detection, segmentation and classification," *Computerized Medical Imaging and Graphics*, vol. 89, p. 101886, Apr. 2021, doi: 10.1016/j.compmedimag.2021.101886.

[5] M. Zabin, H.-J. Choi, and J. Uddin, "Hybrid deep transfer learning architecture for industrial fault diagnosis using Hilbert transform and DCNN–LSTM," *The Journal of Supercomputing*, vol. 79, no. 5, pp. 5181–5200, Mar. 2023, doi: 10.1007/s11227-022-04830-8.

[6] A. Asuntha and A. Srinivasan, "Deep learning for lung cancer detection and classification," *Multimedia Tools and Applications*, vol. 79, no. 11–12, pp. 7731–7762, Mar. 2020, doi: 10.1007/s11042-019-08394-3.

[7] Y. Jiao, J. Li, C. Qian, and S. Fei, "Deep learning-based tumor microenvironment analysis in colon adenocarcinoma histopathological whole-slide images," *Computer Methods and Programs in Biomedicine*, vol. 204, p. 106047, Jun. 2021, doi: 10.1016/j.cmpb.2021.106047.

[8] P. Dutande, U. Baid, and S. Talbar, "LNCDS: a 2D-3D cascaded CNN approach for lung nodule classification, detection and segmentation," *Biomedical Signal Processing and Control*, vol. 67, p. 102527, May 2021, doi: 10.1016/j.bspc.2021.102527.

[9] G. Kasinathan and S. Jayakumar, "Cloud-based lung tumor detection and stage classification using deep learning techniques," *BioMed Research International*, vol. 2022, no. 1, Jan. 2022, doi: 10.1155/2022/4185835.

[10] T. Vaiyapuri, Liyakathunisa, H. Alaskar, R. Parvathi, V. Pattabiraman, and A. Hussain, "Cat swarm optimization-based computer-aided diagnosis model for lung cancer classification in computed tomography images," *Applied Sciences*, vol. 12, no. 11, p. 5491, May 2022, doi: 10.3390/app12115491.

[11] B. Muthazhagan, T. Ravi, and D. Rajinigirinath, "An enhanced computer-assisted lung cancer detection method using content based image retrieval and data mining techniques," *Journal of Ambient Intelligence and Humanized Computing*, Jun. 2020, doi: 10.1007/s12652-020-02123-7.

[12] M. Ragab, H. A. Abdushkour, A. F. Nahhas, and W. H. Aljedaibi, "Deer hunting optimization with deep learning model for lung cancer classification," *Computers, Materials & Continua*, vol. 73, no. 1, pp. 533–546, 2022, doi: 10.32604/cmc.2022.028856.

[13] S. Dlamini, Y.-H. Chen, and C.-F. Jeffrey Kuo, "Complete fully automatic detection, segmentation and 3D reconstruction of tumor volume for non-small cell lung cancer using YOLOv4 and region-based active contour model," *Expert Systems with Applications*, vol. 212, p. 118661, Feb. 2023, doi: 10.1016/j.eswa.2022.118661.

[14] P. Marentakis *et al.*, "Lung cancer histology classification from CT images based on radiomics and deep learning models," *Medical & Biological Engineering & Computing*, vol. 59, no. 1, pp. 215–226, Jan. 2021, doi: 10.1007/s11517-020-02302-w.

[15] P. M. Shakeel, M. A. Burhanuddin, and M. I. Desa, "Automatic lung cancer detection from CT image using improved deep neural network and ensemble classifier," *Neural Computing and Applications*, vol. 34, no. 12, pp. 9579–9592, Jun. 2022, doi: 10.1007/s00521-020-04842-6.

[16] R. Mohana Priya and P. Venkatesan, "An efficient image segmentation and classification of lung lesions in pet and CT image fusion using DTWT incorporated SVM," *Microprocessors and Microsystems*, vol. 82, p. 103958, Apr. 2021, doi: 10.1016/j.micpro.2021.103958.

[17] R. Manickavasagam and S. Selvan, "Automatic detection and classification of lung nodules in CT image using optimized neuro fuzzy classifier with cuckoo search algorithm," *Journal of Medical Systems*, vol. 43, no. 3, p. 77, Mar. 2019, doi: 10.1007/s10916-019-1177-9.

[18] H. C. Reis, V. Turk, K. Khoshelham, and S. Kaya, "MediNet: transfer learning approach with MediNet medical visual database," *Multimedia Tools and Applications*, vol. 82, no. 25, pp. 39211–39254, Oct. 2023, doi: 10.1007/s11042-023-14831-1.

[19] M. A. Talukder, M. M. Islam, M. A. Uddin, A. Akhter, K. F. Hasan, and M. A. Moni, "Machine learning-based lung and colon cancer detection using deep feature extraction and ensemble learning," *Expert Systems with Applications*, vol. 205, p. 117695, Nov. 2022, doi: 10.1016/j.eswa.2022.117695.

[20] J. Civit-Masot, A. Bañuls-Beaterio, M. Domínguez-Morales, M. Rivas-Pérez, L. Muñoz-Saavedra, and J. M. Rodríguez Corral, "Non-small cell lung cancer diagnosis aid with histopathological images using explainable deep learning techniques," *Computer Methods and Programs in Biomedicine*, vol. 226, p. 107108, Nov. 2022, doi: 10.1016/j.cmpb.2022.107108.
[21] S. Mehmood *et al.*, "Malignancy detection in lung and colon histopathology images using transfer learning with class selective image processing," *IEEE Access*, vol. 10, pp. 25657–25668, 2022, doi: 10.1109/ACCESS.2022.3150924.
[22] E. A.-R. Hamed, M. A.-M. Salem, N. L. Badr, and M. F. Tolba, "An efficient combination of convolutional neural network and LightGBM algorithm for lung cancer histopathology classification," *Diagnostics*, vol. 13, no. 15, p. 2469, Jul. 2023, doi: 10.3390/diagnostics13152469.
[23] T. Saikia, R. Kumar, D. Kumar, and K. K. Singh, "An automatic lung nodule classification system based on hybrid transfer learning approach," *SN Computer Science*, vol. 3, no. 4, p. 272, Jul. 2022, doi: 10.1007/s42979-022-01167-0.
[24] M. M. Khan, A. S. Omee, T. Tazin, F. A. Almalki, M. Aljohani, and H. Algethami, "A novel approach to predict brain cancerous tumor using transfer learning," *Computational and Mathematical Methods in Medicine*, vol. 2022, pp. 1–9, Jun. 2022, doi: 10.1155/2022/2702328.
[25] I. Abderrahmane, B. Hadjira, A. Mehadji, and R. Bachir, "High performance single mode plasmonic filter and efficient wavelength demultiplexing based on nanodisk resonators," *Optical and Quantum Electronics*, vol. 55, no. 5, p. 413, May 2023, doi: 10.1007/s11082-023-04673-4.

BIOGRAPHIES OF AUTHORS

Manaswini Pradhan received B.E. in computer science and engineering, M.Tech in computer science from Utkal University, Odisha, India, and Ph.D. degree in the field of information and communication technology from Fakir Mohan University, Odisha. Currently she is working as an assistant professor in P.G. Department of Information and Communication Technology, Fakir Mohan University, Orissa, India. She has been in the teaching profession for the last eighteen, and during this period she also has acquired research experience in the area of artificial neural network, data-mining, and other topics in the broad subject of information and communication technology. She has been awarded research projects by Department of Science and Technology, Government of India, and UGC, New Delhi. She has a published research papers in national and international journals, a book chapter published by Taylor & Francis, Springer, IBI Global and presented papers in various conferences. She is involved in guiding M.Tech/M.Phil computer science scholars in the field of data mining, neural networks, bio-informatics, and application of ICT in healthcare management. She has had shorter stays at several Computing Departments in China, USA, and UAE. Her research aptitude and acumen is of very high order. She can be contacted at email: mpradhan.fmu@gmail.com.

Ahmed Alkhayyat received the B.Sc. degree in electrical engineering from AL KUFA University, Najaf, Iraq, in 2007 and the M.Sc. degree from the Dehradun Institute of Technology, Dehradun, India, in 2010. He contributed in organizing several IEEE conferences, workshop, and special sessions. He is currently a dean of international relationship and manager of the world ranking in the Islamic University, Najaf, Iraq. To serve his community, he acted as a reviewer for several journals and conferences. His research interests include network coding, cognitive radio, efficient-energy routing algorithms and efficient-energy MAC protocol in cooperative wireless networks and wireless local area networks, as well as cross-layer designing for the self-organized network. He can be contacted at email: ahmedalkhayyat85@gmail.com.